Bioactive Materials 44 (2025) 82–96

Contents lists available at ScienceDirect

Bioactive Materials

journal homepage: www.keaipublishing.com/en/journals/bioactive-materials

Nano-based perivascular intervention sustains a nine-month long-term suppression of intimal hyperplasia in vein grafts

Takuro Shirasu [a,b,1], Go Urabe [a,c,1], Nisakorn Yodsanit [d,1], Yitao Huang [a,1], Ruosen Xie [d], Matthew S. Stratton [e], Matthew Joseph [f], Zhanpeng Zhang [d], Yuyuan Wang [d], Jing Li [a], Runze Tang [a], Lynn M. Marcho [g], Li Yin [h], Eric W. Kent [a], Kaijie Zhang [h], Ki Ho Park [a], Bowen Wang [a,h], K. Craig Kent [a,***], Shaoqin Gong [d,i,**], Lian-Wang Guo [a,j,*]

[a] Division of Surgical Sciences, Department of Surgery, School of Medicine, University of Virginia, Charlottesville, VA, 22908, USA
[b] Division of Vascular Surgery, Department of Surgery, The University of Tokyo, Tokyo, 113-8655, Japan
[c] Division of Vascular Surgery, Sakakibara Heart Institute, Fuchu, Tokyo, 183-0003, Japan
[d] Department of Biomedical Engineering and Wisconsin Institute for Discovery, University of Wisconsin-Madison, Madison, WI, 53715, USA
[e] Department of Physiology and Cell Biology, The Ohio State University, Columbus, OH, 43210, USA
[f] Interventional Cardiology Cath Core Lab, Davis Heart & Lung Research Institute, The Ohio State University, Columbus, OH, 43210, USA
[g] Division of Medical Oncology, The Ohio State University Comprehensive Cancer Center, 420 W. 12th Ave., Columbus, OH 43210, USA
[h] Department of Surgery, Feinberg School of Medicine, Northwestern University, Chicago, IL 60603, USA
[i] Department of Ophthalmology and Visual Sciences, University of Wisconsin-Madison, Madison, WI, 53715, USA
[j] Department of Molecular Physiology and Biological Physics, School of Medicine, University of Virginia, Charlottesville, VA 22908, USA

ARTICLE INFO

Keywords:
Post-surgery failure of open vascular reconstructions
Intimal hyperplasia
Vein graft
Arteriovenous fistula
Perivascular drug delivery
Pericelle
Long-term efficacy

ABSTRACT

Open vascular reconstructions (OVR), including bypass grafts and dialysis access, are standard treatments for cardiovascular and renal diseases. Unfortunately, OVR often fail largely due to intimal hyperplasia (IH), and there are no clinical methods to prevent this complication. Perivascular drug administration during OVR presents a promising strategy for IH suppression. However, durations of drug release from carriers are generally short whereas sustained efficacy is essential for clinical success. This raises a critical question in clinical translation: can IH suppression be realistically maintained long-term (e.g., over 6 months) with short-term perivascular interventions? To address this question, we modified a rat vein-graft model to prolong IH progression. We then applied Pericelle, a nanoparticle/hydrogel hybrid system that we developed for perivascular delivery of rapamycin, an established IH-inhibitory drug. Surprisingly, despite short (~3-month) drug release, Pericelle demonstrated IH suppression throughout 3, 6, and 9 months with IH reduced from 115.58 ± 27.89 to 40.34 ± 5.18 at 9 months ($P < 0.05$, $n = 6$ rats), as indicated by morphometric analysis. Live animal ultrasonography showed the same trend. Consistently, histone-3 lysine-27 trimethylation, an epigenetic mark associated with IH progression, was decreased at 6 months after Pericelle treatment. Moreover, Pericelle exhibited promising efficacy in mitigating IH in a porcine model of arteriovenous fistula that mimics dialysis access. These results suggest that Pericelle-mediated suppression of IH in rat vein-grafts extends much beyond drug release, offering potential solutions to longstanding translational challenges in reducing OVR failure.

1. Introduction

Occlusive vascular diseases are a major cause of death worldwide. [1]. Among these, coronary and peripheral artery diseases hold particular prevalence, often requiring invasive interventions such as bypass grafting, endovascular angioplasty, and endarterectomy. [2]. Bypass grafting serves as the only and "last stand" treatment for left main

Peer review under responsibility of KeAi Communications Co., Ltd.
* Corresponding author.
** Corresponding author.
*** Corresponding author.
E-mail address: lg8zr@virginia.edu (L.-W. Guo).
[1] co-first authors.

https://doi.org/10.1016/j.bioactmat.2024.10.005
Received 25 March 2024; Received in revised form 1 September 2024; Accepted 3 October 2024
Available online 13 October 2024

Abbreviations

AVF	arteriovenous fistula
CCA	common carotid artery
DLS	dynamic light scattering
EC	endothelial cells
H3K27me3	histone-3 lysine-27 trimethylation
HPLC	high-performance liquid chromatography
IEL	internal elastic lamina
IH	intimal hyperplasia
mTOR	mammalian target of rapamycin
NP	unimolecular nanoparticle
OVR	open vascular reconstructions
PAMAM	poly(amidoamine)
PEG	poly(ethylene glycol)
PLGA	poly(lactic acid-co-glycolic acid)
pS6RP	phospho-S6 ribosomal protein
PSV	Peak systolic velocity
SMC	smooth muscle cells

coronary artery disease, three-vessel coronary artery disease, and extensive peripheral artery disease, etc., with over 400,000 cases performed each year in the US alone. [1,3]. Autologous vein grafts stand as the most reliable and commonly used vascular conduits. [2]. Furthermore, hemodialysis serves as a lifeline for patients with end-stage renal disease, with arteriovenous fistula (AVF) considered the optimal method of vascular access, surpassing arteriovenous grafting, subcutaneously fixed superficial arteries, and permanent vascular catheters. [4]. These surgical procedures, including bypass grafting, dialysis access, and endarterectomy, herein collectively referred to as open vascular reconstructions (OVR) due to their requirement for open-body surgery, amount to over a million cases each year in the US alone. [4,5]. Unfortunately, post-procedure failure rates are unacceptably high (e.g. bypass initial year 15–50 %), inflicting tremendous human and financial costs. [2,6]. Despite numerous studies, there remains an absence of approved methods to prevent post-surgery failure of OVR aside from standard post-operative care with aspirin and statins. [7,8].

Intimal hyperplasia (IH) is a common etiology for the post-surgery failure of OVR. This process engenders a new layer of tissue on the inner vessel wall occupying the lumen space. [2,9,10]. Numerous attempts have been made to inhibit IH in bypass grafts via systemic drug treatments, e.g., clopidogrel, ticlopidine, vitamin K antagonists, rivaroxaban, omega-3 fatty acids fish oil, and cilostazol. [2,4,8,9]. But none has resulted in a clinical use, most likely owing to systemic toxicity and limited duration of the therapeutics. Alternative to systemic treatments, perivascular drug delivery is an attractive route particularly suitable for OVR, taking advantage of accessibility to the exposed vessel during the surgery. [10–14]. This approach allows for the use of various drug carriers and maximizes the local concentration of the drug while limiting its leak into the circulation. [12,14]. Clinical trials have involved rapamycin-impregnated polymer mesh, vascular endothelial growth factor (VEGF)-expressing adenovirus in collagen collars, and rapamycin-eluting collagen wrap, etc. [14,15], but none has become a clinical method [12]. Preclinical studies testing drug-releasing gels, wraps, microneedles, and cuffs have shown efficacy yet with various limitations such as physical stress on the vessel and short-term efficacy. [12,14,16,17].

In recent years, there has been a growing utilization of microparticles and nanoparticles (NPs) for perivascular therapeutic delivery. [13,16,18–23]. NPs offer a multitude of advantages, including their adaptability, multifunctionality, and minimal mass which imposes little physical stress on the vessel [13]. In previous studies [19], we developed a NPs/hydrogel hybrid system, subsequently named Pericelle (patent US10668017B2). In this prototype product, the model drug rapamycin, known for its clinical efficacy in preventing restenosis in stents implanted post-angioplasty, is encapsulated within unimolecular micelle NPs. These NPs are formed by single multiarmed-star amphiphilic block copolymers with exclusively covalent bonds, demonstrating excellent rapamycin-loading capacity and in vivo stability [19]. The drug-loaded NPs are suspended in a thermosensitive poly(lactic acid-co-glycolic acid)−poly(ethylene glycol)−poly (lactic acid-co-glycolic acid) (PLGA-PEG-PLGA) triblock hydrogel (referred to as triblock gel), which remains as a pre-gel solution when kept on ice. Upon perivascular application, this liquid undergoes a phase transition into a paste, effectively confining the drug-loaded NPs to the targeted vessel. This NPs/gel combination, named Pericelle, outperforms either NPs or triblock gel alone by providing a sustained rapamycin release over approximately 3 months [19]. In a rat model of injury-induced acute IH, perivascular application of Pericelle significantly inhibited IH at 3 months post-injury without affecting reendothelialization [19]. These results suggest the potential utility of Pericelle in preventing IH-associated failure of OVR.

However, achieving even longer efficacy would be imperative for the clinical use of Pericelle or other products, particularly considering that IH progresses over 1–18 months following the initial surgery of human vein grafting. [24,25]. It is a common challenge to translate preclinical findings from acute preclinical models into long-term clinical benefits, primarily due to two major barriers. First, disease phenotypes such as IH often regress in acute models, limiting the ability to assess long-term therapeutic effects. [20]. Second, drug carriers composed of natural or synthetic materials are inevitably subject to decomposition in the body, resulting in limited drug release durations. [19]. Indeed, perivascular drug delivery to mitigate IH has been seldom explored in studies lasting over three months. [19,26,27]. Despite technological advancements, reports of long-term release (defined herein as over 6 months) of a drug contained within a polymer carrier have been extremely rare. [28,29]. From this perspective, an important unanswered question arises: can perivascular drug delivery for a short term realistically have an IH-mitigating effect over a long term? Addressing this question is crucial for bridging the knowledge gap in translational research and advancing the development of effective treatments for IH in clinical practice.

In the current study, we tackled this longstanding question regarding the sustained inhibition of IH. We introduced a modification to a rat vein-graft model, enabling the observation of IH progression for at least 6 months post-grafting. This allowed us to evaluate Pericelle's efficacy for 12 months. Remarkably, despite the relatively short release duration of rapamycin from Pericelle (~3 months [19]), we observed a sustained IH-inhibitory effect lasting 9 months in rat vein grafts treated with Pericelle. In our mechanistic investigation, we found that Pericelle treatment led to a reduction in histone-3 lysine-27 trimethylation (H3K27me3), a chromatin mark associated with the progression of IH. [30,31]. To further explore the translational potential of Pericelle, we tested it in a porcine AVF model, and the results further supported Pericelle's IH-inhibitory effect. Overall, our findings implicate the potential of Pericelle to bridge the gap in translational research by offering long-term efficacy in mitigating IH.

2. Materials and methods

2.1. Materials

Rapamycin was purchased from LC Laboratories (Woburn, MA). Fourth generation Poly(amidoamine) (PAMAM) dendrimer was purchased from NanoSynthons, LLC (Mt. Pleasant, MI). Dimethyl sulfoxide (DMSO), δ-valerolactone (VL) were purchased from Sigma-Aldrich (St. Louis, MO). mPEG−COOH (Mn = 5 kDa) was acquired from JenKem Technology (Allen, TX, USA). All other reagents were purchased from Thermo Fisher Scientific (Waltham, MA, USA) unless otherwise specified. The purity of reagents is listed in Table S1.

2.2. Preparation and characterization of rapamycin-loaded nanoparticles

Unimolecular micelle nanoparticles (herein denoted as NPs) were prepared as we described before. [19]. In brief, PAMAM−PVL-OH was synthesized through ring-opening polymerization of δ-valerolactone (VL) at 120 °C using PAMAM−OH G.4 (50 mg) as a macroinitiator, VL (673 mg, 640 μL) as a monomer, and $Sn(Oct)_2$ (2.283 μL) as a catalyst. PAMAM−PVL−PEG was then produced by conjugating mPEG−COOH (94.8 mg) to PAMAM-PVL-OH (20 mg) via an esterification reaction.

To prepare drug-loaded NPs, PAMAM−PVL−PEG (100 mg) and rapamycin (30 mg) were dissolved in DMF followed by a dropwise addition of DI water (DMF: DI water = 1:3 vol ratio). The solution was then dialyzed via a cellulose membrane dialysis tubing (molecular weight cutoff, 15 kDa) against DI water for 48 h and lyophilized. The rapamycin-loaded NPs were characterized as we previously reported. [19]. Briefly, polymer chemical structures were determined using ^1H NMR spectroscopy, and their molecular weights were measured by gel permeation chromatography (GPC). The rapamycin-loading level in the NPs (20 % loading content of rapamycin in NP) and its release rate were quantified by high-performance liquid chromatography (HPLC). The morphologies of the NPs were determined by dynamic light scattering (DLS, Zetasizer Nano ZS90, Malvern Instrument) and transmission electron microscopy (TEM, FEI Tecnai G2 F30 TWIN 300 kV, E.A. Fischione Instruments, Inc.). Consistent with our previous report [19], the average hydrodynamic diameter of the NPs in an aqueous solution was around 83.4 nm with PDI = 0.190, as measured by DLS (Fig. S1 and Table S2), and the average diameter of dried NPs was around 35 nm, as measured by TEM from previous work [19]. Furthermore, release profiles were determined in vitro (see our previous report [19]). Rapamycin directly dispersed in a triblock hydrogel (described below) without using NPs showed a profile of burst release that completed at ~30 days. In contrast, rapamycin-loaded NPs suspended in the triblock gel exhibited a superior sustained (~3–4 months) rapamycin release profile. [19].

2.3. Synthesis of thermo-sensitive triblock hydrogel

The PLGA−PEG−PLGA triblock gel was prepared as previously described. [19]. Briefly, hydroxyl-terminated PEG (2.4 g) was dried under vacuum at 120 °C for 2 h. Lactide (5.0 g) and glycolide (1.2 g) were then added and vacuum-dried at 70 °C for 30 min. Upon complete melting of the mixture, a catalyst amount of $Sn(Oct)_2$ ($[Sn(Oct)_2]/[LA + GA]$ = 1:500 mol/mol) was added, and polymerization proceeded at 150 °C for 8 h. The resultant mixture was dissolved in cold water (4 °C) and precipitated at 80 °C. The precipitation process was repeated three times to purify the co-polymers which, as the final product, were lyophilized.

2.4. Preparation and in vivo application of pericelle

The PLGA−PEG−PLGA triblock copolymers were dissolved in water (23 % by weight) at 4 °C, resulting in a pre-gel solution of the triblock gel. The rapamycin-loaded, lyophilized NPs were added to ice-cold PBS buffer and then suspended in the triblock gel solution contained within a microcentrifuge tube, which was kept on ice. When transferred from the tube onto a grafted vein or arteriovenous fistula (AVF), Pericelle, the triblock gel containing NPs, rapidly solidified, transforming into a paste, which was then spread to uniformly coat all sides of the graft.

2.5. Animals used for surgeries

All animal experiments complied with the *Guide for the Care and Use of Laboratory Animals* (National Institutes of Health), and the protocols are approved by the Institutional Animal Care and Use Committee of The Ohio State University (Columbus, Ohio). Male Sprague-Dawley rats were purchased from Charles River Laboratories (Wilmington, MA), and kept in isolation racks in an air-conditioned room with 12 h light-dark cycle, fed with a normal diet, and free to access food and water. The rats of 10–11 weeks old at 330–350 g were used for surgery. The experiments using farm pigs were performed in The Ohio State University Interventional Cardiology Cath Core Lab (Manager: Matthew Joseph).

2.6. Modified vein-graft model for long-term studies

Interposition vein-graft surgeries were performed using a cuff technique as described [32–34] with minor modifications. The cuffs were cut from a 20-gauge intravenous catheter (BD InsyteTM, BD, Franklin Lakes, NJ). The rat was kept anesthetized via inhalation of 2–2.5 % of isoflurane/oxygen flow. A saline solution of 100 units of heparin was injected subcutaneously. The external jugular vein was carefully dissected, collected, and stored in a heparin saline solution (50 U/ml) after gently flushing its lumen with the same solution. The proximal and distal ends of the remaining vein were ligated.

The right common carotid artery was dissected, ligated in the middle, and then transected in between the two ligated sites. The cuff was slipped over the proximal common carotid artery (CCA) and secured in place by clamping its handle, and the open end of the CCA was everted over and tied to the cuff. The same procedures were repeated for the distal CCA. The vein-graft was then sleeved over the cuffed arterial ends, and the vein-artery connections were secured with sutures. The blood flow was resumed, and the internal carotid artery (ICA) and external carotid artery (ECA) were both ligated at the previously looped sites, leaving only the occipital artery and the superior thyroid artery open for restricted blood flow. After confirmation of graft patency, 3 mg of Pericelle with 20 wt % of rapamycin (equivalent to 600 μg) loaded in the NPs was applied around the graft. Since the purpose of the experiment is to test the therapeutic effect of Pericelle as the whole product, vein-grafts in the control group of rats were generated without applying Pericelle. The neck incision was then closed. The rat was kept in a clean cage with a warming pad until fully recovered and the pain was controlled by subcutaneous administration of Buprenorphine.

Forty-eight rats were randomly allocated to either the control or Pericelle groups. In each group, the 24 rats were randomly assigned for the post-surgery endpoint of 3, 6, 9, or 12 months (6 rats in each subgroup). One rat in the Pericelle 9-month subgroup had occlusion in the vein-graft at 6 months. Another rat in the control 12-month subgroup died in the 38th week with an unknown cause.

2.7. Creation of porcine AVFs and perivascular application of pericelle

Arteriovenous fistulas (AVFs) were created according to previous descriptions. [35,36]. Briefly, the anesthesia of farm pigs was induced with an intramuscular injection of ketamine (15 mg/kg) and midazolam (0.2 mg/kg) and maintained with inhalation of 2–3% isoflurane. The preoperative analgesics buprenorphine (0.005 mg/kg) and carprofen (4 mg/kg) and the broad-spectrum antibiotic Excede (5 mg/kg, Zoetis, Parsippany, NJ) were given intramuscularly. All surgical procedures including perivascular drug application were conducted under sterile conditions. Through the 8–10 cm longitudinal skin incisions just caudal to the inguinal ligaments, femoral veins (~6 mm in diameter) were dissected with ligations of all visible tributaries. We then designed the anastomosis 2 cm proximal to the assumed end of the femoral veins. Femoral arteries (~4 mm in diameter) were dissected only at the site of anastomosis and clamped. After the dissection of bilateral femoral arteries and veins, we prepared arteries for anastomosis by soaking in the mixed solutions of 10 ml of 2 % lidocaine and 10 ml of 0.5 % bupivacaine for 5 min. Pigs were heparinized with an initial dose of 5000 USP plus 1000 USP every hour. Side-to-end anastomoses were created with 6-0 Surgipro™ sutures (Covidien, Dublin, Ireland). After completion of anastomoses, the patency of AVFs were confirmed with palpitation of thrill and/or auscultation of bruit.

After the creation of bilateral AVFs and confirmation of hemostasis,

we applied Pericelle containing 2–4 mg rapamycin in the NPs around the left-side AVF, leaving the right-side AVF without Pericelle treatment. Surgicel (Ethicon Inc) was used to underlie the gel. To prevent its migration, the gel was loosely wrapped inside Surgicel. Postoperative courses were uneventful except for percutaneous drainage of fluid collection on the right side in two pigs. In another experiment, we tested the usefulness of Tisseel (fibrin sealant, Baxter International Inc., Deerfield, IL) in 2 pigs as an equivalent of the triblock gel used in Pericelle. We dispersed the rapamycin-containing NPs in Tisseel and applied it around the left side AVF leaving the right side AVF without treatment.

2.8. Postoperative cares and euthanasia of pigs

Oral Carprofen (4 mg/kg) was administered postoperatively for 3 days. Pigs were administered with aspirin EC 325 mg one day before surgery until post-surgery day 28. Omeprazole (40 mg BID) and Sucralfate (1g) were given from day 1 through day 28. We examined the patency on day 7, 14, and 28 by auscultation and ultrasound. At the time of euthanasia on day 28, intra-arterial angiography was performed via the left common carotid artery. After systemic injection of 10000 USP heparin, pigs were euthanized, and bilateral AVFs were harvested *en bloc* to include 3 cm proximal to the anastomosis. Lumens were gently flushed with saline to remove the residual blood. The AVFs were fixed in 10 % neutral buffered formalin for 48 h and then dehydrated in 70 % ethanol. The specimens were cut at the anastomosis and 4 mm intervals towards the downstream of the veins, as previously described [36]. The first 3 blocks (proximal) beyond the anastomosis (juxta-anastomotic region) were considered to be exposed to perivascularly applied Pericelle.

Upon the application of Pericelle in rats and pigs, we determined the rapamycin drug doses based on our and others' reports. We previously used Pericelle containing 600 μg rapamycin per rat, a dose that effectively reduced IH in a carotid arterial injury model [19]. In the current study, we used the same dose for rat vein grafts. For pig AVF experiments, we referenced a report using a dose of 60 μg rapamycin per cm^{-2} that mitigated IH in a pig vein graft model [26]. Based on the outer surface areas covered by Pericelle on rat vein grafts and pig AVFs, we estimated that the local concentrations of rapamycin in these models were within the range of 50–100 $\mu g/cm^2$.

2.9. Ultrasonography with live animals

We examined the vein-grafts by ultrasound imaging (Vevo 3100, FUJIFILM VisualSonics, Toronto, Canada) at different time points after surgery. The rats were anesthetized with 5 % of isoflurane in a chamber and then maintained at 2–3% of isoflurane in a supine position on the Vevo imaging station during imaging. The graft was detected by the MX550D transducer (25–55 MHz) and quantified at three quartile points between two cuffs. Parameters of peak systolic velocity, lumen diameter, and total graft wall thickness were measured at each quartile point.

2.10. Morphometric analysis of intimal hyperplasia in rat vein-grafts

At each time point (specified in figure legends), the rats were anesthetized with 2–2.5 % isoflurane and perfused with phosphate-buffered saline followed by 4 % paraformaldehyde (PFA) at a physiological pressure of 100 mm Hg. The animals were then euthanized. The grafts were collected and fixed in 4 % PFA overnight. Then, grafts were chopped into three portions of the same length: proximal, middle, and distal. Paraffin sections (5 μm thick) were excised from these vein segments at 100 μm intervals and then Van Gieson-stained for morphometric analysis of proximal and distal portion of the grafts. We used Image-J to measure the area inside the internal elastic lamina (IEL), IEL perimeter, and lumen perimeter. Morphometric parameters were calculated as follows: Intima area (IEL area - lumen area), normalized intima area (intima area/IEL length), and stenosis rate (intima area/IEL area). As vein-graft samples are flabby, the lumen space tends to collapse compromising lumen area quantification. To circumvent this problem for more accurate measurement, we calculated lumen area mathematically using lumen perimeter which is not affected by the shape of the lumen. Measurements were performed by a researcher blinded to the experimental conditions using 3-4 sections from each of the proximal and distal segments of the graft. The data from all sections were pooled to generate the mean for each animal. The means from all animals were then averaged, and the standard error of the mean (SEM) was calculated.

2.11. Immunofluorescence on vein-graft cross-sections

The assay was conducted according to our previously reported protocol [37]. In brief, cross-sections of veins or vein-grafts were incubated overnight in cold room with an antibody specific to H3K27me3 [38] (Cat#9733, Cell Signaling Technology, Danvers, MA, USA) or phospho-S6 ribosomal protein (pS6RP, phosphorylation at Ser235/236, Cat#2211, Cell Signaling Technology, Danvers, MA, USA). The sections were then rinsed and incubated with an anti-rabbit secondary antibody conjugated with Alexa Fluor 594 (A-11037, Invitrogen, Carlsbad, CA). DAPI was used to stain the nuclei. Images of the specific staining of H3K27me3 was captured with the EVOS M7000 cell imaging system (Thermo Fisher Scientific). Quantification was performed using ImageJ. For each animal, 4–5 immunostained cross-sections were used. The values from all cross-sections were pooled to generate the mean for each animal. The means from all animals in each group were then averaged, and the final mean ± SEM was calculated.

2.12. Histological analysis of AVFs

The collected specimens were embedded in paraffin, cut transversely at 4 μm thickness, and stained with the Verhoeff-Van Gieson method. Morphometric analysis was conducted using Image J software (NIH, Bethesda, MD, USA). Fresh thrombus was excluded from IH measurement as previously described. [36]. Lumen area (A_1), the length or perimeter of the abluminal border of media (L), and the area surrounded by this border (A_2) were determined. Intima + media area (IM area) and IM thickness (or normalized IM area) were calculated as A_2-A_1 and (A_2-A_1)/L, respectively. The raw stenosis rate was (A_2-A_1)/A_2. Since veins are prone to distortion and compression, we corrected the stenosis rates based on the perimeter (L). The corrected stenosis rate was calculated as (IM area)/(L*L/4/π). Values from each block were used for statistical analysis.

2.13. Mass spectrometry determination of rapamycin retention after pericelle application

Under general anesthesia with 2–2.5 % of isoflurane inhalation and through a midline incision in the neck, the left sternocleidomastoid muscle and omohyoid muscle were resected, and the left CCA was dissected for Pericelle application. The rats were randomly assigned to 2 treatment groups: intravenous injection (600 μg free naked rapamycin via right external jugular vein, n = 8) or perivascular treatment with Pericelle [600 μg rapamycin in NPs dispersed in 400 μL of triblock hydrogel). Four rats of each group were euthanized with overdose anesthesia on day 14, and the other four on day 28. After perfusion with phosphate-buffered saline, the left carotid arteries were harvested for tissue concentration analysis of rapamycin.

Tissue samples were extracted by pre-weighing tissue before adding 100 μL of methanol per mg of tissue, 2 μL of internal standard per 100 μL of MeOH and then sonicating the extraction mixture for 20 cycles of 30-s on/off sonication with a Biorupter® (Diagenode, Denville, NJ). The samples were then centrifuged and aliquoted into LC vials for quantification. Calibration solutions were prepared by creating standards of rapamycin from 1.0 ng/mL up to 10000 ng/mL in pure water or MeOH

and protein precipitate or incubated with samples before running, depending on which sample type was being run.

UltiMate 3000 HPLC (Thermo Fisher Scientific) was used. A 5 μL sample was injected for every run. We used H_2O with 0.1 % formic acid as Solvent A and 100 % MeOH as Solvent B. Column was Poroshell 120 SB-C18 (2 × 100 mm, 2.7 μm particle size). The flow rate was set at 200 μL/min, and the column temperature was maintained at 38 °C. The gradient began with an initial flow rate of 2 % solvent B for 3 min, then a linear ramp to 45 % B at 12.5 min, 90 % B from min 14 to min 18, down to 20 % at 20 min, and back to 2 % B from 25 min and equilibration of 2 % B until 30min.

The samples were quantified using a heated electrospray ionization source on a TSQ Quantiva triple-stage quadrupole mass spectrometer (Thermo Fisher Scientific) at The Ohio State University Mass Spec and Proteomics Facility. For rapamycin, the transition monitored was precursor 936.6 *m/z* and product 409.29 *m/z* and collision energy of 25 V, while the internal standard ascomycin was monitored from 809.5 *m/z* to 756.39 *m/z* at 16 V, and everolimus was monitored at the transition from 975.6 *m/z* to 908.5 *m/z* at 16 V. For all experiments, the capillary voltage was set to 4.0 kV with a capillary temperature of 350 °C, a vaporizer temperature of 100 °C, a sheath gas of 10, and auxiliary gas of 8.

2.14. Statistical analysis

Values are presented as mean ± standard error of the mean (SEM). Statistical analysis was conducted using unpaired Student *t-tests*, multiple *t-tests*, one-way analysis of variance (ANOVA), or otherwise specified. Data are considered statistically significant if a P value is < 0.05.

3. Results

3.1. A modified rat vein graft model enables the progression of IH throughout 6 months

In traditional acute models, such as arterial injury in rodents, IH typically stops progressing approximately one month after surgery [20], posing limitations for long-term translational research. Longer IH progression can be observed in rat vein-to-artery grafting models. However, the neointimal morphology is often eccentric, thin, and highly variable [39–42], complicating IH data interpretation.

To address these challenges, we adopted a modification of the model originally proposed by Jiang et al., who induced augmented IH in New Zealand White rabbits by completely ligating the distal internal carotid artery (ICA) and partially ligating the external carotid artery (ECA) at the time of vein implantation. [34]. In our modified model, we fully ligated both the ECA and ICA, thereby restricting blood flow to only the thin occipital artery and superior thyroid artery (Fig. 1A and B). We then morphologically characterized the vein grafts at three time points (1, 3, and 6 months). Remarkably, the neointimal tissue appeared relatively even, concentric, and thick, especially on the proximal side of the vein graft (Fig. 1C; for the distal side, see Fig. S2). Most importantly, we observed a trend of continuous increase in IH over the 6-month period following grafting (Fig. 1D). Significant differences ($P < 0.05$) were found in the normalized intima area on both the proximal side (3–6 months) and distal side (1–6 months), as well as in the stenosis rate on both sides (1–6 months and 3–6 months for proximal side; 1–3 months and 1–6 months for distal side). Thus, our modified rat vein graft model enables continuous progression of IH for at least 6 months, facilitating long-term studies (herein denoted as >6 months).

3.2. Morphometric analysis indicates the long-term effectiveness of pericelle for IH mitigation in rat vein grafts

We were thus able to test the therapeutic effect of Pericelle on IH for 12 months. As depicted in Fig. 1E, rapamycin served as the model drug, which was harbored inside the hydrophobic core of the unimolecular NPs. The rapamycin-loaded NPs were then dispersed in the triblock hydrogel (kept as a pre-gel solution in a microcentrifuge tube on ice). [19]. The rapamycin release was determined to be ~3 months as we previously reported [19]. When transferred onto the outer surface of the vein graft, the hydrogel became a paste (Fig. 1F), which sequestered the NPs in the perivascular space yet without physically impinging on the vessel.

Since neither the triblock gel alone nor the unimolecular NPs affected IH, as previously determined [19], herein our focus shifted to evaluating the long-term efficacy of Pericelle, the NPs/gel combination as a complete product, particularly with consideration for future clinical translation. Accordingly, Pericelle was applied to vein-grafts in one group of rats, while vein-grafts in another group served as untreated controls without Pericelle. A total of forty-eight rats were randomly assigned to the 3-, 6-, 9-, or 12-month groups, with each subgroup comprising 6 rats and receiving either saline or Pericelle treatment.

Fig. 2 displays morphometric parameters, with IH represented by the intima area normalized to the internal elastic lamina (IEL) perimeter which is a measurement unaffected by morphological distortions (for full-view cross-sections, see Fig. S3). On the proximal side, Pericelle treatment reduced IH from 126.68 ± 7.92 to 75.06 ± 5.04 after 3 months, from 176.21 ± 16.07 to 119.61 ± 16.10 after 6 months, and from 115.58 ± 27.89 to 40.34 ± 5.18 after 9 months. Accordingly, the stenosis rate decreased from 35.74 ± 3.02 to 20.66 ± 2.04 after 3 months, from 47.89 ± 4.36 to 33.86 ± 5.81 after 6 months, and from 34.9 ± 5.52 to 15.02 ± 2.26 after 9 months. The data of intima area without normalization showed the same trend (Fig. S4A). The media area was not altered by Pericelle treatment (Fig. S4B).

The values for IH and stenosis rate in the middle and distal portions of the grafts largely mirrored those observed in the proximal side at 3, 6, and 9 months, although with varying statistical outcomes. At 12 months, no significant differences in IH or stenosis rate were found, except for a difference in distal stenosis rate (Fig. 2B). Over the 12-month period, a trend toward increased lumen area was observed in the Pericelle groups compared to the control groups. Statistical significance was reached at 6 months for the proximal side and at 12 months for the middle and distal portions. The overall size of the graft (adventitia perimeter) remained unchanged by Pericelle treatment at either time point (Fig. S5).

Thus, perivascular treatment with Pericelle effectively mitigated IH at least for 9 months in rat vein grafts following graft surgery.

3.3. Ultrasonography reveals a trend of IH mitigation by pericelle treatment

Shown in Fig. 3 are ultrasonographic parameters, which could be conveniently recorded for the whole graft (proximal, middle, and distal). Fig. 3A and B illustrate how these parameters were measured. Total wall thickness is an excellent parameter to noninvasively determine possible therapeutic effects by using live animals. We found that there was a general trend of decrease in total wall thickness at 3, 6, and 9 months after initial surgery, in Pericelle-treated groups *vs* the control groups. The Pericelle-*vs*-control differences were significant ($P > 0.05$) at 6 months in all the proximal, middle, and distal portions and at 3 months in the proximal and distal portions, but not at 9 months and 12 months. If compared within the control groups, total wall thickness increased from 3 months to 6 months (Fig. 3C). Peak systolic velocity (PSV) tends to increase at the narrowed vessel site. We observed that PSV was decreased by Pericelle at 3 months and 6 months ($P = 0.063$) in the middle portion of the grafts and at 12 months on the distal side (Fig. 3D). Lumen diameter showed a trend of increase in Pericelle-treated groups *vs* controls throughout 12 months in the whole graft but with no statistical significance (Fig. S6). Thus, the result of total wall thickness measured via ultrasonography is overall consistent with the inhibitory effect of Pericelle on IH measured by morphometry.

To confirm that the drug rapamycin could truly diffuse into the graft

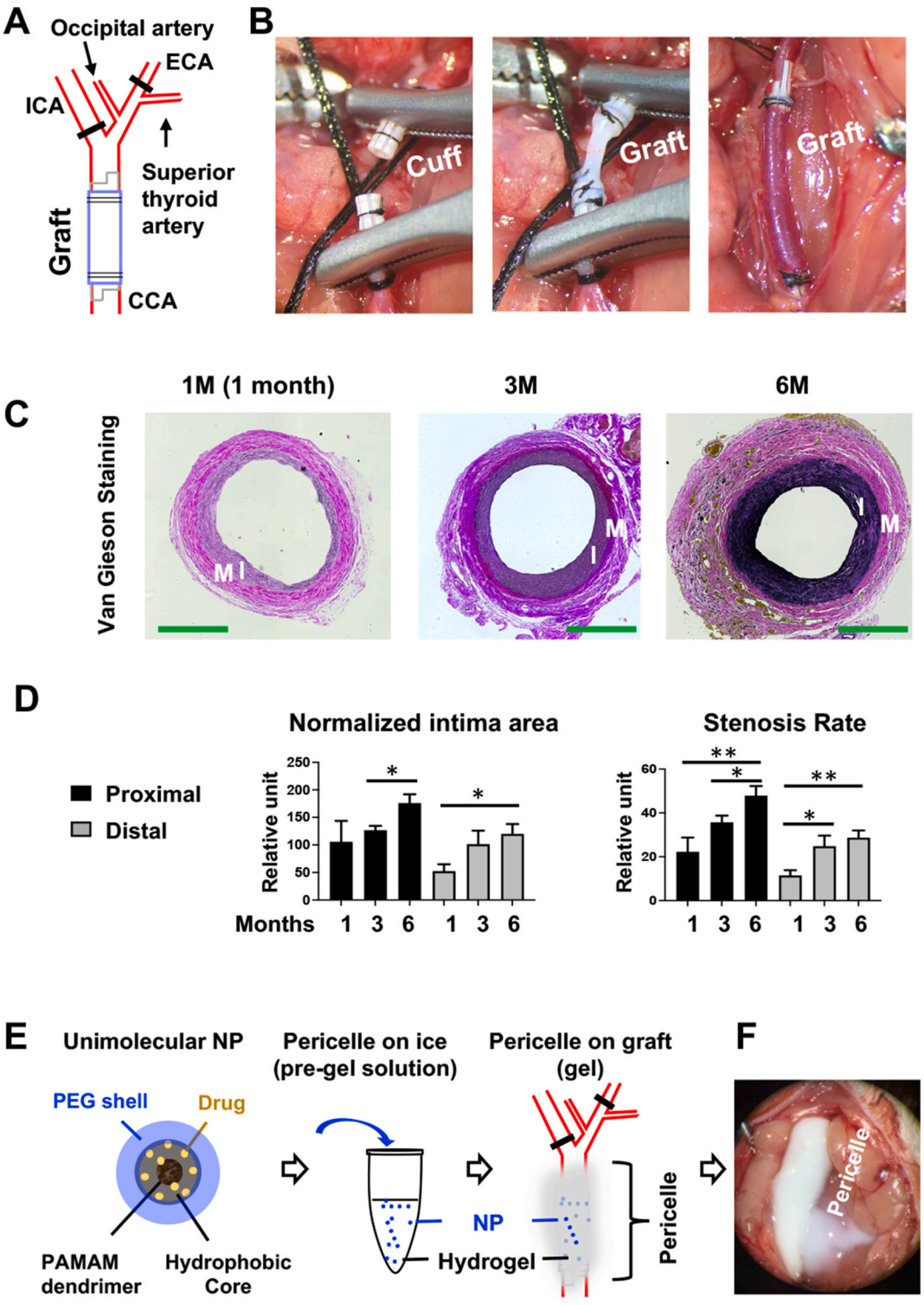

Fig. 1. A modified rat vein-graft model exhibits prolonged IH progression.
Vein-grafts were created in Sprague-Dawley rats by completely ligating both the internal carotid artery (ICA) and external carotid artery (ECA) to restrict blood flow. This method represents a modification of the previously reported technique used in rabbits, where only the ICA was completely ligated while the ECA was partially ligated. A. Schematic of the modified vein-graft model using the interposition cuff technique. Both ICA and ECA are ligated, leaving only occipital and superior thyroid arteries open for blood flow. B. Pictures showing the procedures of interposition grafting of the jugular vein to the common carotid artery in rats. C. Representative Van Gieson-stained cross-sections from the vein-graft proximal side. I, intima. M, media. Scale bar: 500 μm. D. Quantification: The values from multiple sections were pooled to generate the mean for each portion of the graft (proximal or distal) in each animal. The means from all animals in each time-point group were then averaged, and the final mean (±SEM) was calculated (n = 5 rats). Multiple *t*-test for pairwise comparison: *p < 0.05, **P < 0.01. E. Schematic. The unimolecular NP has a core-shell structure. While the hydrophobic core provides high drug-loading capacity, the hydrophilic PEG shell renders the NP highly soluble and readily dispersible in the triblock hydrogel, which is a pre-gel solution on ice but becomes a paste at body temperature. F. Representative picture showing perivascular application of Pericelle which is the white paste on the rat vein-graft.

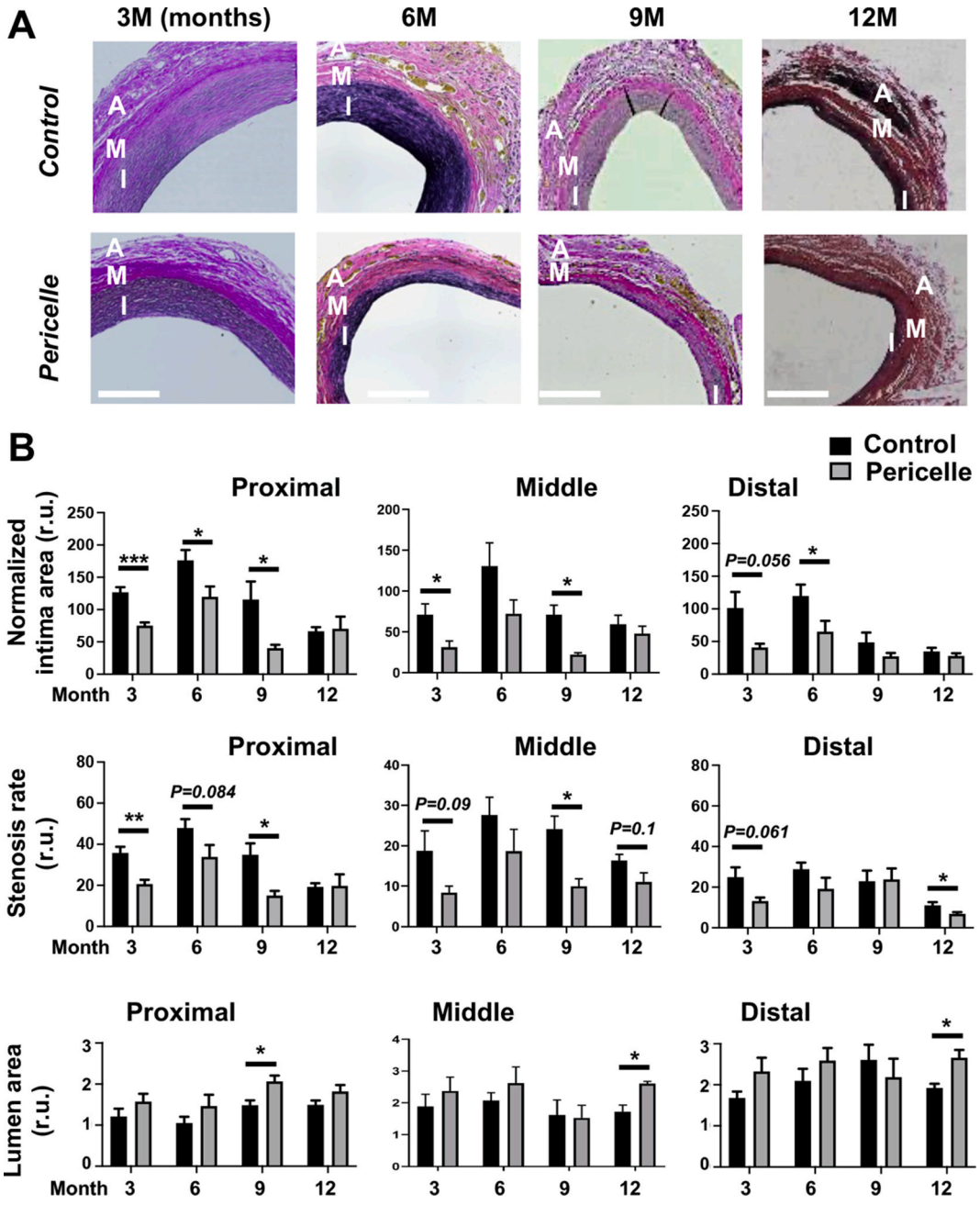

Fig. 2. Long-term inhibition of vein-graft IH by Pericelle.
Jugular vein to common carotid artery interposition grafting was performed in Sprague-Dawley rats. To determine the effect of Pericelle as a whole product on IH and to mimic clinical translation, Pericelle was applied onto vein-grafts in one group of rats leaving the vein-grafts in the other group of rats untreated (saline control). Morphometric analysis was performed on Van Gieson-stained vein-graft sections.
A. Representative van Gieson-stained vein-graft sections. A, adventitia. M, media. I, intima. Bar: 200 μm
B. Quantification. The values from multiple sections were pooled to generate the mean for each portion of the graft (proximal, middle, or distal) in each animal. The means from all animals in each group were then averaged, and the final mean (±SEM) was calculated (n = 6 rats). Multiple t-tests for pairwise comparison: *p < 0.05, **P < 0.01, ***P < 0.001.

wall, we determined the tissue concentration of rapamycin in the vessel tissues by mass spectrometry (Fig. S7). The tissue concentrations appeared high at 14 and 28 days after perivascular application of Pericelle, in contrast to the near-zero concentrations after intravenous injection of free rapamycin of the same dosage, although a statistical significance was not found possibly due to data variability. This result nonetheless supports the drug availability in the vessel wall after Pericelle application.

To determine whether rapamycin persisted in the grafts until 3 months, we extracted small molecules from tissue sections. Mass spectrometry analysis revealed no detectable rapamycin remaining in the tissue (Fig. S8). Given the potential loss of rapamycin during the paraffin section preparation that may confound the result, we employed an alternative approach. We used reduction of pS6RP, a key downstream effector of mammalian target of rapamycin (mTOR), as an indicator of rapamycin's inhibitory effect on mTOR [43,44]. Immunofluorescence analysis of vein graft sections indicated a reduction in pS6RP at 3 months (Fig. 4A), but not at 6 (Fig. 4B) or 9 months (Fig. S9) after Pericelle treatment. This in vivo observation, consistent with our in vitro data showing ~3–4 months of rapamycin release [19], suggests that

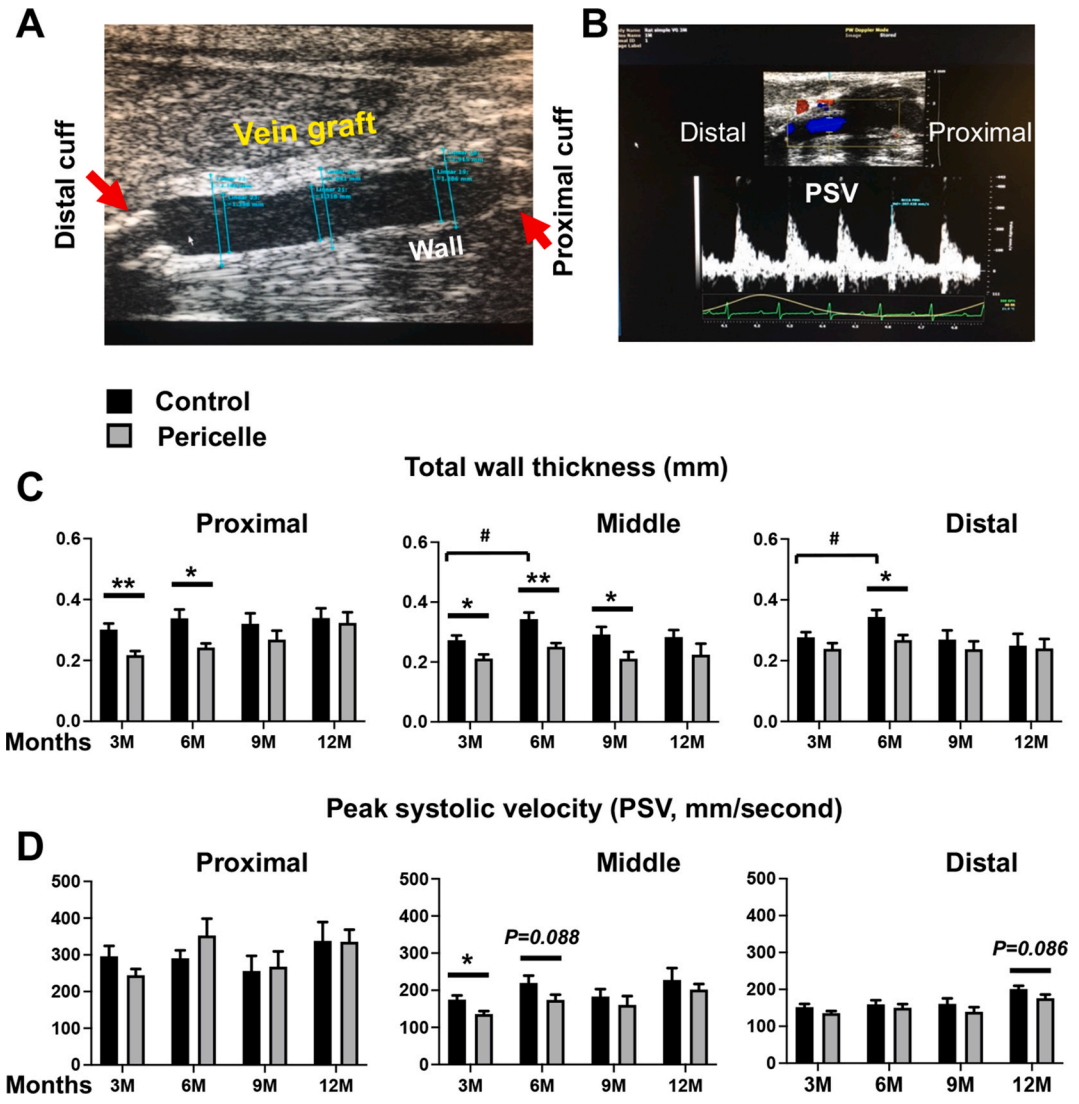

Fig. 3. Ultrasonographic measurement of the effect of Pericelle on vein-graft IH. Ultrasonography was performed with live animals at each time point before their euthanization for morphometric analysis.

A. Representative still picture of ultrasonography for the measurement of vein-graft wall thickness (longitudinal view). Arrows point to the cuffs used for the interposition grafting surgery.

B. Representative still picture of ultrasonography for the measurement of peak systolic velocity.

C. and D. Quantification. Data are presented as mean ± SEM (n = 6 rats). Pairwise comparisons were conducted using multiple t-tests, with significance denoted as follows: *p < 0.05, **P < 0.01. #P < 0.05.

rapamycin remained available in the grafts at 3 months but not much longer, likely in residual amounts considering the high efficacy of this drug. These results confirm the limited in vivo duration of rapamycin/Pericelle while highlighting its long-term inhibitory effect on IH (at least 9 months, see Fig. 2B).

Taken together, the above findings demonstrate that Pericelle is an effective perivascular delivery system that produces long-term efficacy of IH mitigation for rat vein grafts.

3.4. Upregulation of IH-associated histone mark H3K27me3 is observed in vein-grafts, which is suppressed by pericelle treatment

IH is a complex process of vascular wall remodeling that involves multiple cell types including smooth muscle cell (SMC), endothelial cell (EC), and immune cells [45,46]. This remodeling is closely associated with epigenetic dysregulation [47,48]. We previously observed a surge of the histone-3 mark H3K27me3 in rat arteries that underwent injury-induced IH [49], a finding further elaborated in others' and our reports [38,50]. Tamping down H3K27me3 reduced IH [31,38,50]. However, whether H3K27me3 upregulation occurs in vein grafts remained unknown. To address this, we conducted immunostaining for H3K27me3 on cross-sections of vein-grafts. As seen in Fig. 5A, H3K27me3 levels in grafted veins markedly increased at 1 month after grafting and remained high at 3 months and 6 months compared to that in the veins without grafting (0 month). This result indicates an upregulation of H3K27me3 in vein-grafts associated with IH.

To investigate a potential epigenetically related mechanism underlying the IH-mitigating effect, we assessed the impact of Pericelle on H3K27me3 levels. Since our data showed a robust inhibitory effect of Pericelle on IH at 6 months, determined either by histology or ultrasound imaging (Figs. 2 and 3), we chose this time point for immunostaining of H3K27me3 on vein-graft sections. We found that Pericelle treatment lowered vein-graft H3K27me3 substantially (Fig. 5B). This observation of rapamycin/pericelle inhibiting H3K27me3 in vein-grafts represents a novel finding not previously reported.

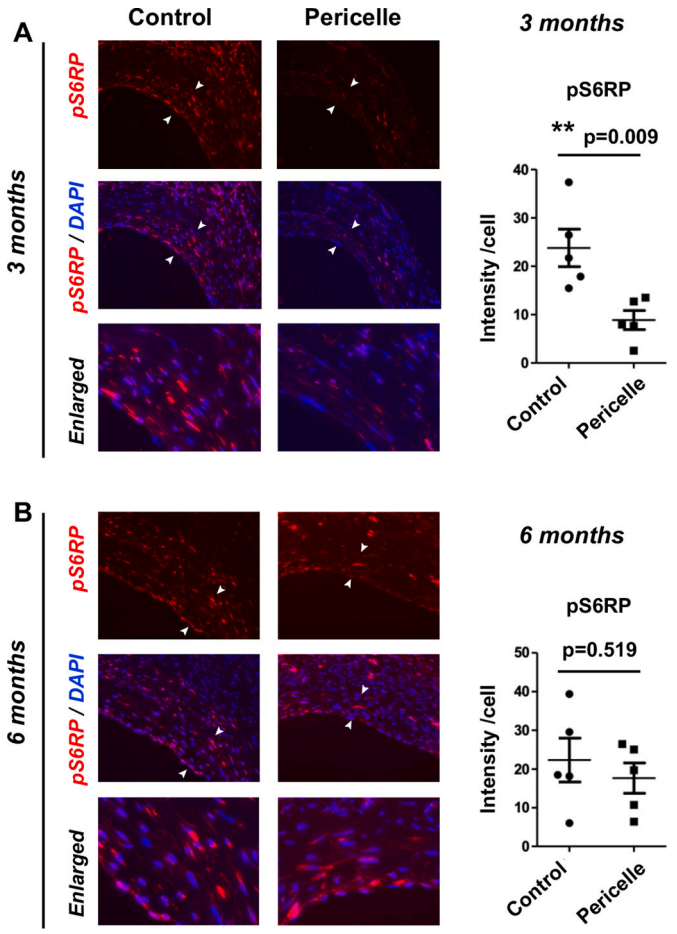

Fig. 4. Effect of Pericelle on reducing pS6RP levels in rat vein grafts.
Jugular vein to common carotid artery interposition grafting was performed in Sprague-Dawley rats. Immunofluorescence staining of pS6RP was conducted on the cross-sections of vein-grafts collected at 3 months (A) and 6 months (B). For quantification, the values from multiple sections were pooled to generate the mean for each animal. The means from all animals in each group were then averaged, and the final mean (±SEM) was calculated. Student t-test: $^{**}p < 0.01$, n = 5 rats. Arrows demarcate the intimal thickness.

3.5. Pericelle treatment does not exert fibrogenic toxicity on rat vein-grafts

During the 12-month study period, we monitored natural weight gain in both control and Pericelle-treated groups of rats, without observing a significant difference in body weight between the two groups (Fig. S10). This suggests the absence of systemic toxicity associated with the perivascular application of Pericelle.

Next, we investigated vein graft fibrosis, a commonly used indicator of vascular tissue toxicity. As depicted in Fig. 6, Pericelle treatment did not lead to increased collagen deposition in the graft wall. Rather, Pericelle significantly reduced collagen deposition at 6 months compared to the control group. This result suggests a potential protective effect of Pericelle against vein graft fibrosis, further supporting its safety profile in vascular tissues.

3.6. Pericelle reduces IH in the porcine model of AVF

Testing therapeutic interventions in large animal models is crucial for translating preclinical successes into clinically useful treatments. Moreover, there exists a similarity between vein grafts and AVFs in their IH pathobiology. [4,51]. We were thus motivated to test Pericelle on porcine AVFs. Following the methods outlined by the Roy-Chaudhury group [35,36], we generated femoral AVFs (Fig. 7A) on both sides of the pig and applied Pericelle onto the left-side AVF but not the right-side AVF. Ultrasonography revealed patent AVF arteries and veins throughout the 4-week observation period, although the blood flow in the veins appeared turbulent compared to that in the arteries (Fig. 7B). After 4 weeks, the pigs were euthanized, and the patency of the fixed veins and arteries was confirmed (Fig. 7C).

Angiography further confirmed the patency of the AVF veins and arteries. Notably, while control veins exhibited narrowed sites, the Pericelle-treated veins appeared smoother and more homogeneous (Fig. 8A). Morphometric analysis revealed a reduction in IH in the Pericelle group compared to controls, with a 62.9 % decrease in IM (I + M) area, a 47.3 % decrease in IM thickness, and a 21.1 % reduction in stenosis rate (Fig. 8B and C). To assess whether the triblock gel in Pericelle uniquely facilitated the IH-mitigating therapeutic effect, we also tested Tisseel, a fibrin sealant commonly used in clinical practice to control bleeding, as a carrier for rapamycin-containing NPs (Fig. S11). However, both angiography and morphometric analyses showed no difference in IH between NPs/Tisseel and the control (Fig. S11). Thus, the combination of NPs/triblock gel (Pericelle) but not NPs/Tisseel for rapamycin delivery was effective in reducing IH in porcine AVFs.

4. Discussion

Our major finding is that mitigation of IH in rat vein-grafts can be sustained at least for 9 months via perivascular application of Pericelle, despite its rapamycin-release duration of only ~3 months. This finding challenges the conventional perception that IH mitigation would cease once drug release completes. Whereas the inevitable decomposition of drug carriers limits drug release to relatively short periods [28,29], long-term efficacy is important for clinical applications. This reality has seemingly dashed the hope of translating preclinical successes into long-term clinical benefits. Indeed, despite numerous preclinical discoveries, there is a persistent translational gap in attaining long-term efficacy of perivascular treatment of IH [3,14]. Currently, there are no approved clinical methods to prevent post-surgery failure of OVR. [6,51]. Hence, a critical question arises: Can long-term IH suppression be realistically achievable through short-term perivascular treatments? Unfortunately, there has been a lack of research specifically addressing this question. In this context, the achievement of 9-month IH mitigation via Pericelle in our study represents a significant breakthrough.

The sustained IH-inhibitory efficacy of Pericelle for 9 months (Fig. 2) is somewhat surprising, considering the limited duration of its ~3-month drug release [19] (Fig. 4). To our knowledge, this is the first report of mitigating vein-graft IH for such an extended duration via perivascular drug delivery. Previous studies have demonstrated IH reduction at 6 months post-surgery in pigs and baboons through the external application of polymer stents, although these did not include a drug component. [52–54]. Additionally, inhibition of IH for 6 months was observed in rabbits through ex vivo delivery of oligo gene therapy to saphenous vein-grafts. [55,56]. Despite these findings and the PREVENT clinical trials [8,15], no clinical treatments have materialized. [2,57]. It is noteworthy that our perivascular drug treatment utilized a nanoparticle/hydrogel system, a strategy markedly different from those employed in these previous studies.

The exact mechanism underlying the observed long-term efficacy resulting from short-term drug release in our study remains unclear at present. However, it can be rationalized considering the major molecular and cellular events that drive IH in vein grafts. First, the dissection and severing of the vein during harvesting impose physical trauma [58]. Second, vascular cells within the harvested vein experience ischemic damage during the period before grafting. [58]. Third, the grafted vein is subject to transient ischemia, high arterial pressure, and shear stress, all contributing to EC and SMC damage, as well as disruption of tight junctions between ECs. [59]. This leads to exposure of the underlying basement membrane rich in collagen, promoting platelet accumulation

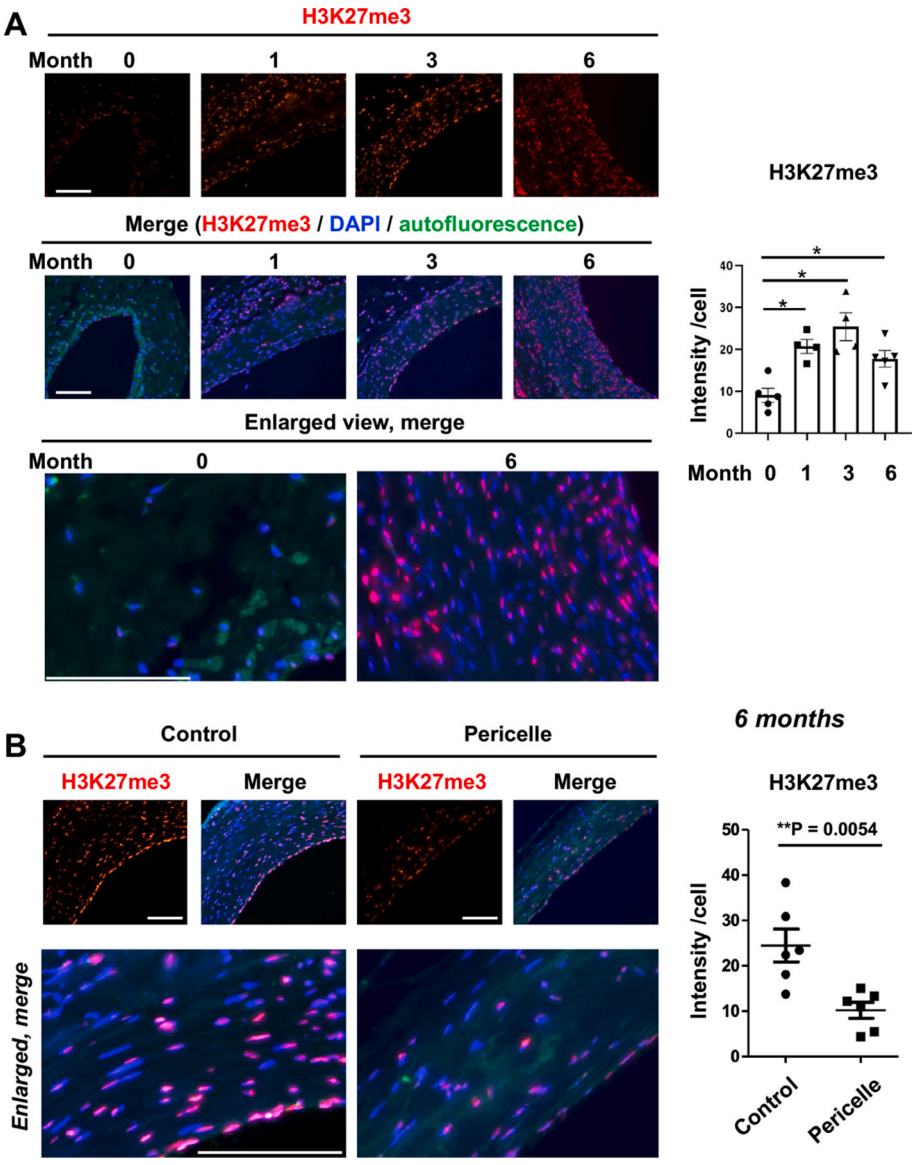

Fig. 5. Effect of Pericelle on H3K27me3 levels in rat vein grafts.
Jugular vein to common carotid artery interposition grafting was performed in Sprague-Dawley rats. Immunofluorescence staining of H3K27me3 was conducted on vein-graft sections. For quantification, the values from multiple sections were pooled to generate the mean for each animal. The means from all animals in each group were then averaged, and the final mean (±SEM) was calculated.
A. Upregulation of H3K27me3 in vein-grafts. A, adventitia. M, media. I, intima. Bar: 200 μm. Zero month refers to the veins that were not grafted. Statistical analysis: ANOVA/Dunnett's test: *$p < 0.05$, $n = 5$ rats.
B. Inhibition of H3K27me3 by Pericelle. Vein-graft sections were collected 6 months after grafting. Statistical analysis: Student t-test: **$p < 0.01$, $n = 6$ rats.

and subsequent recruitment of immune cells, which produce large amounts of pro-inflammatory cytokines. [2]. In such a pathogenic environment, SMCs and ECs along with other cells transform into pro-inflammatory and IH-forming cells, perpetuating inflammation and IH in a vicious cycle. [25,59].

There is evidence indicating that the activation of pro-IH signaling pathways and rapid progression of IH occur mainly in the initial 1–3 months in the rabbit saphenous vein-graft model [34,60], largely agreeing with that observed in rat and pig vein-graft models. [26,36,61,62]. It is thus plausible to infer that disrupting the early phase pro-IH vicious cycle, even for a relatively short period, could have an extended effect on the later progression of IH. Supporting this notion, our previous research has demonstrated that perivascular delivery of rapamycin using nanoparticles in Pluronic gel, with an estimated drug release of approximately 1–2 weeks, resulted in IH mitigation at 4 weeks post-surgery in an acute IH model of arterial injury in rats. [20]. In human saphenous vein-grafts, the postoperative 1–12 months represent the most active period of IH development, accounting for graft failure rates ranging from 15 % to 50 %. [24,63]. From this perspective, we speculate that the 9-month efficacy observed with Pericelle in rats may be potentially extendable to cover the fast-growing phase of IH occurring within the 1–12 month postoperative period in human vein-grafts. This suggests that the short-term intervention provided by Pericelle holds promise for yielding long-lasting benefits in curbing IH progression in clinical settings.

It is interesting to note that the difference in IH between the Pericelle and control groups disappeared at 12 months. This phenomenon could be ascribed to either the regression of IH, which would minimize the difference between the groups, or the cessation of the therapeutic effect. Given that IH began to regress after 6 months in the rat vein-graft model, we were unable to discern between these two scenarios. Consequently, we are not able to determine whether the IH-abating effect of Pericelle

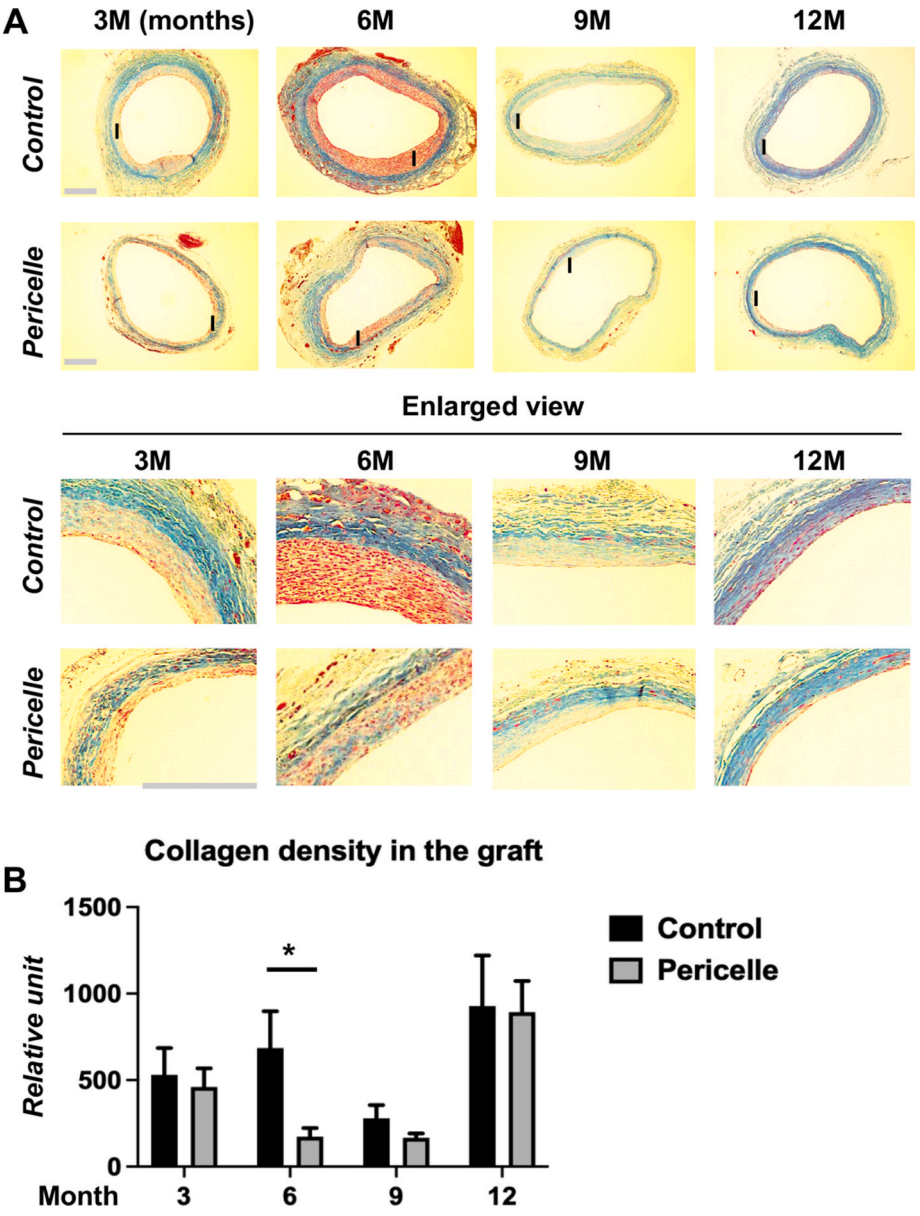

Fig. 6. Effect of Pericelle on collagen density in the vein-graft wall. Mason's trichrome staining was performed with vein-graft cross-sections.
A. Representative stained sections. I, intima. Bar: 200 μm
B. Quantification. The values from multiple sections of different locations (proximal, middle, distal) were pooled to generate the mean for each animal. The means from all animals in each treatment group were then averaged, and the final mean (±SEM) was calculated (n = 6 rats). Multiple t-tests for pairwise comparison: *p < 0.05.

could last for even longer (>9 months) if a longer-term IH model would be available. It is therefore important to continue the research using a vein-graft model that more closely mimics human vein-grafts with progressive IH. Obese Zucker rats, which bear human-like diseases such as diabetes mellitus and hypercholesterolemia [64], may serve this purpose. Nevertheless, to our knowledge, this is the first study to demonstrate the therapeutic benefit of IH mitigation for a 9-month long duration via perivascular drug delivery in a vein-graft model. Thus, our study provides valuable insights and is encouraging as it suggests the feasibility of achieving prolonged IH-mitigating therapeutic efficacy using polymer delivery tools such as Pericelle despite limited drug release time.

As demonstrated by our tests using the porcine AVF model, Pericelle has the potential to be applied to AVFs, especially considering fistularized veins and the high risk of IH in fistula failure. [4,51]. Since hemodialysis is essential to replace kidney function in patients with end-stage renal disease, AVF failure can jeopardize a patient's quality of life and even pose life-threatening risks. [4,9]. Despite reported primary patency rates of 50%–70 % at one year, AVFs often deteriorate in the course of hemodialysis, particularly at the anastomosis or due to repetitive punctures. [9]. IH is a major contributor to AVF failure, alongside other factors such as early thrombosis, inadequate vessel diameters, poor inflow or run-off, and infection. [10,21]. Therefore, the prevention of IH in AVF is an urgent challenge. Several therapeutic trials have been performed, and antineoplastic, anti-inflammatory, and antithrombotic agents are the most auspicious. [4]. However, achieving a perivascular treatment that offers long-term effectiveness in preventing AVF failure remains an unmet clinical need. Further development of Pericelle for this purpose is therefore warranted.

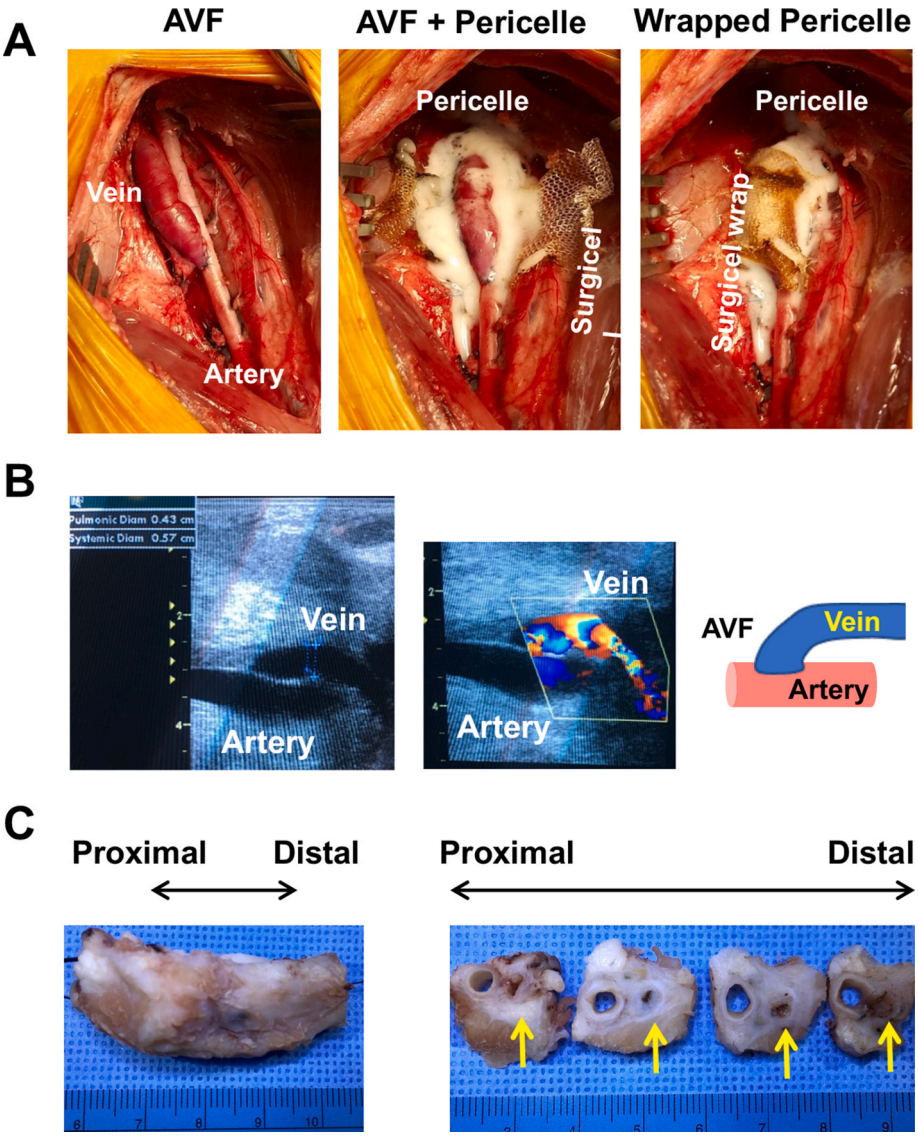

Fig. 7. Application of Pericelle to the porcine model of AVF. Femoral arterio-venous fistula (AVF) was generated in farm pigs.
A. Pictures showing the completed AVF, perivascular application of Pericelle (white paste) around the AVF, and loose wrapping of Pericelle with Surgicel to prevent migration of the gel.
B. Representative still pictures of ultrasonography (longitudinal view). The left picture shows the patency of the AVF. The superimposed image (middle) illustrates turbulent blood flow in the AVF vein. On the right, a cartoon explains the orientations of the vein and artery that form the AVF.
C. Fixed tissue block of AVF. The cross-sections of the AVF artery and vein were cut at different locations of the block. Arrows points to the vein which appears patent. The AVF was collected 4 weeks after the surgery and Pericelle application.

4.1. Study limitations

The current study has several limitations that merit consideration for future studies. Pericelle could serve as a perivascular delivery platform for testing other IH-inhibitory drugs either individually or as a mixture of NPs loaded with different agents. Candidate drugs like UNC1999 or EED226, known for effectively reducing H3K27me3 and mitigating IH in an injury-induced rat model [31,38,49,50], could be explored in future investigations. Our in vivo data indicate that rapamycin-containing Pericelle lowers H3K27me3 levels in rat vein grafts, consistent with previously observed effects of rapamycin on H3K27me3 in cancer cells [65]. These observations suggest a potential crosstalk between the mTOR pathway and chromatin remodeling, warranting further exploration. Recent discoveries suggest that the histone mark H3K27me3 and its associated "epigenetic memory" can persist across mitotic generations, maintaining cell phenotypic traits [66]. Our data also show sustained H3K27me3 upregulation in rat vein grafts for at least six months, accompanied by the prolonged H3K27me3-suppressing effect of Pericelle treatment. This raises intriguing questions as to whether epigenetic memory (H3K27me3 and suppression thereof) contributes to the extended efficacy of Pericelle. While Pericelle offers advantages in targeting the perivascular space, future studies should monitor potential drug leakage into the bloodstream. Moreover, research using animal models that more closely replicate human disease conditions which do not regress, such as obese Zucker rats [64] for the vein-graft model, could provide further insights. Extending testing to large animals, like pigs, would also enhance the comprehensive evaluation of Pericelle's translational potential.

5. Conclusions

A longstanding question in translational research pertains to whether short-term perivascular treatments can yield prolonged inhibition of IH. In this study, we present the first evidence demonstrating that mitigation

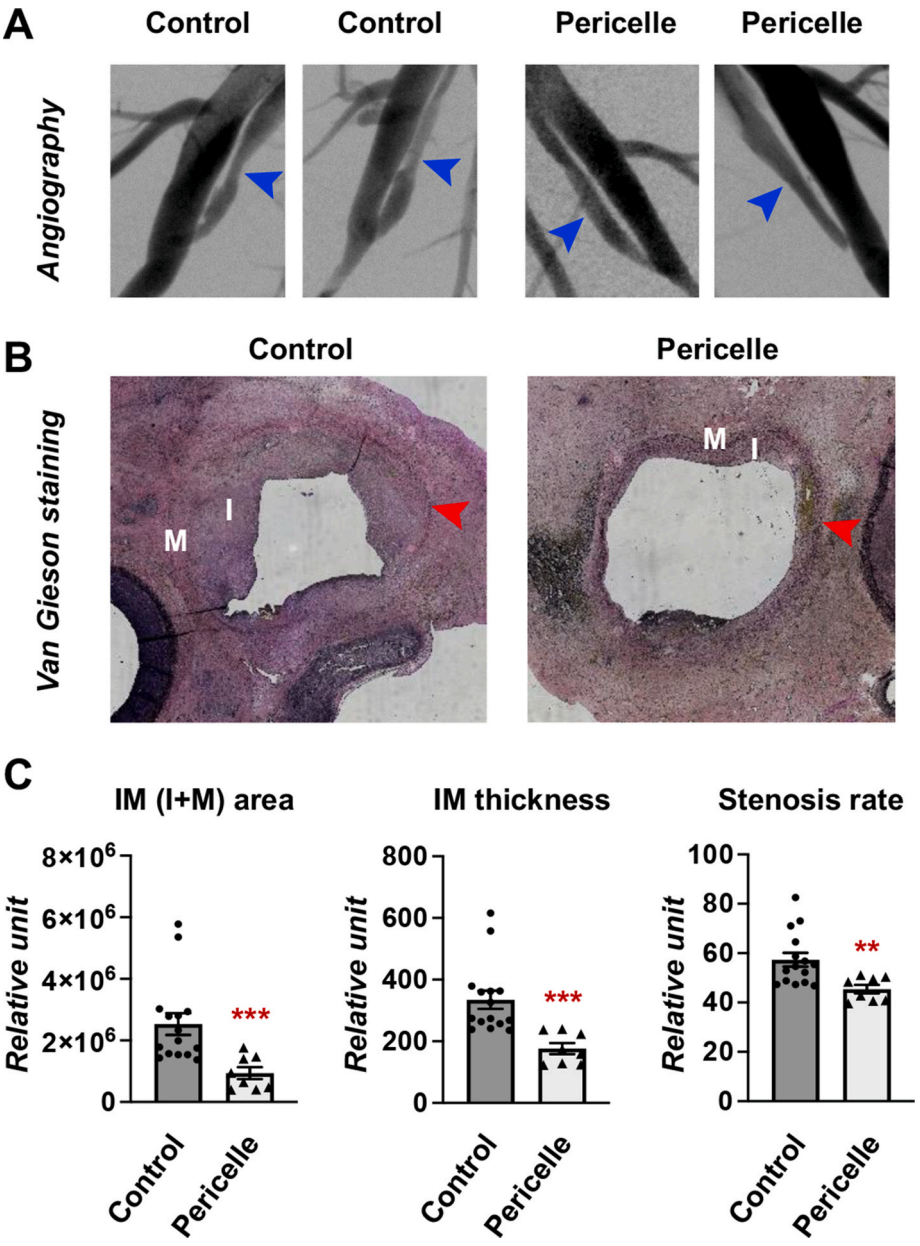

Fig. 8. IH-inhibitory effect of Pericelle on porcine AVFs.
Femoral AVFs were generated on both sides of the pig. Pericelle was applied onto the left-side AVF and the right-side AVF was not treated (saline control). The AVFs were collected 4 weeks after the surgery.
A. Angiography showing compromised patency in controls and normal patency in Pericelle-treated AVFs, as indicated by the blue arrow heads.
B. Representative van Gieson-stained AVF vein cross sections. M, media. I, intima. Red arrowhead demarcates the abluminal border of the media.
C. Quantification. Data are presented as mean ± SEM, which is calculated using the values pooled from multiple AVF vein sections; n = 5 pigs (control) or n = 3 pigs (Pericelle). Unpaired Student t-test: **P < 0.01, ***P < 0.001. IM area refers to the area that contains both intima and media. IM thickness refers to the IM area normalized to the perimeter of the abluminal border of the media (see red arrowhead).

of IH in rat vein-grafts could be extended to 9 months via Pericelle, with this mitigation involving chromatin remodeling and possibly epigenetic memory. Moreover, our findings indicate that Pericelle is effective in reducing IH in a porcine AVF model, further underscoring its potential for clinical translation. Given more than a million OVR cases a year in the US alone, further development of the Pericelle technology is warranted, which may ultimately contribute to improved management of post-surgery failure of OVR.

Ethics approval and consent to participate

All animal experiments complied with the *Guide for the Care and Use of Laboratory Animals* (National Institutes of Health), and the protocols are approved by the Institutional Animal Care and Use Committee of The Ohio State University (Columbus, Ohio).

CRediT authorship contribution statement

Takuro Shirasu: Writing – original draft, Methodology, Investigation, Formal analysis, Data curation. **Go Urabe:** Writing – original draft, Methodology, Investigation, Formal analysis, Data curation. **Nisakorn Yodsanit:** Validation, Methodology, Data curation. **Yitao Huang:** Investigation, Formal analysis, Data curation. **Ruosen Xie:** Methodology. **Matthew S. Stratton:** Supervision, Investigation. **Matthew**

Joseph: Supervision, Resources. **Zhanpeng Zhang:** Methodology. **Yuyuan Wang:** Validation. **Jing Li:** Visualization, Validation, Formal analysis. **Runze Tang:** Visualization. **Lynn M. Marcho:** Methodology. **Li Yin:** Methodology, Resources. **Eric W. Kent:** Resources, Writing – review & editing. **Kaijie Zhang:** Methodology. **Ki Ho Park:** Methodology. **Bowen Wang:** Methodology, Investigation. **K. Craig Kent:** Writing – review & editing, Funding acquisition, Conceptualization. **Shaoqin Gong:** Writing – review & editing, Supervision, Funding acquisition, Conceptualization. **Lian-Wang Guo:** Writing – review & editing, Writing – original draft, Supervision, Project administration, Investigation, Funding acquisition, Conceptualization.

Declaration of competing interest

The authors declare that they have no known competing financial interests or personal relationships that could have appeared to influence the work reported in this paper.

Acknowledgements

This work was supported by the NIH Center for Accelerated Innovations-Cleveland Clinic (NCAI-CC) award 1UH54HL119810-06 (1118-SUB) to K.C.K. and L.-W.G., The Ohio State University Accelerator award (ECG20170069) to K.C.K. and L.-W.G., and the Ohio Development Services Agency fund (GRT00051721) to L.-W.G. This research also partially involved funding support from NIH awards R01HL129785 (to K.C.K., S.G., and L.-W.G.) and R01HL168405 (to L.-W.G., K.C.K., and S.G.).

We thank Dr. Keith Ozaki for instructions on the rat vein graft model, Dr. Prabir Roy-Chaudhury for instructions on the pig AVF model, Dr. Diego Celdran-Bonafonte for detailed technical advice on creating pig AVFs, and Dr. Hosam El Sayed who helped on pig surgery. We also thank Dr. Mark Low at the NIH Center for Accelerated Innovations at Cleveland Clinic (NCAI-CC) for his guidance on this translational project. In addition, we appreciate very much Dr. Guojun Chen's insights during the discussion on revision.

Appendix A. Supplementary data

Supplementary data to this article can be found online at https://doi.org/10.1016/j.bioactmat.2024.10.005.

References

[1] E.J. Benjamin, P. Muntner, A. Alonso, M.S. Bittencourt, C.W. Callaway, A. P. Carson, A.M. Chamberlain, A.R. Chang, S. Cheng, S.R. Das, F.N. Delling, L. Djousse, M.S.V. Elkind, J.F. Ferguson, M. Fornage, L.C. Jordan, S.S. Khan, B. M. Kissela, K.L. Knutson, T.W. Kwan, D.T. Lackland, T.T. Lewis, J.H. Lichtman, C. T. Longenecker, M.S. Loop, P.L. Lutsey, S.S. Martin, K. Matsushita, A.E. Moran, M. E. Mussolino, M. O'Flaherty, A. Pandey, A.M. Perak, W.D. Rosamond, G.A. Roth, U. K.A. Sampson, G.M. Satou, E.B. Schroeder, S.H. Shah, N.L. Spartano, A. Stokes, D. L. Tirschwell, C.W. Tsao, M.P. Turakhia, L.B. VanWagner, J.T. Wilkins, S.S. Wong, S.S. Virani, E. American Heart Association Council on, Prevention statistics C and stroke statistics S. Heart disease and stroke statistics-2019 update: a report from the American heart association, Circulation 139 (2019) e56–e528.

[2] M.R. de Vries, K.H. Simons, J.W. Jukema, J. Braun, P.H. Quax, Vein graft failure: from pathophysiology to clinical outcomes, Nat. Rev. Cardiol. 13 (2016) 451–470.

[3] K.W. Southerland, S.B. Frazier, D.E. Bowles, C.A. Milano, C.D. Kontos, Gene therapy for the prevention of vein graft disease, Transl. Res. 161 (2013) 321–338.

[4] J.H. Lawson, L.E. Niklason, P. Roy-Chaudhury, Challenges and novel therapies for vascular access in haemodialysis, Nat. Rev. Nephrol. 16 (2020) 586–602.

[5] P.P. Goodney, A.W. Beck, J. Nagle, H.G. Welch, R.M. Zwolak, National trends in lower extremity bypass surgery, endovascular interventions, and major amputations, J. Vasc. Surg. 50 (2009) 54–60.

[6] K.M. Trocha, P. Kip, M. Tao, M.R. MacArthur, J.H. Trevino-Villarreal, A. Longchamp, W. Toussaint, B.N. Lambrecht, M.R. de Vries, P.H.A. Quax, J. R. Mitchell, C.K. Ozaki, Short-term preoperative protein restriction attenuates vein graft disease via induction of cystathionine gamma-lyase, Cardiovasc. Res. 116 (2020) 416–428.

[7] K. Solo, S. Lavi, C. Kabali, G.N. Levine, A. Kulik, A.A. John-Baptiste, S.E. Fremes, J. Martin, J.W. Eikelboom, M. Ruel, A.A. Huitema, T. Choudhury, D.L. Bhatt, N. Tzemos, M.A. Mamas, R. Bagur, Antithrombotic treatment after coronary artery bypass graft surgery: systematic review and network meta-analysis, BMJ 367 (2019) l5476.

[8] C.N. Hess, R.D. Lopes, C.M. Gibson, R. Hager, D.M. Wojdyla, B.R. Englum, M. J. Mack, R.M. Califf, N.T. Kouchoukos, E.D. Peterson, J.H. Alexander, Saphenous vein graft failure after coronary artery bypass surgery: insights from PREVENT IV, Circulation 130 (2014) 1445–1451.

[9] E.A. Takahashi, S. Kilari, S. Misra, Novel clinical therapies and technologies in dialysis vascular access, Kidney 2 (2021) 1373–1379.

[10] C. Zhao, S.T. Zuckerman, C. Cai, S. Kilari, A. Singh, M. Simeon, H.A. von Recum, J. N. Korley, S. Misra, Periadventitial delivery of simvastatin-loaded microparticles attenuate venous neointimal hyperplasia associated with arteriovenous fistula, J. Am. Heart Assoc. 9 (2020) e018418.

[11] B. Wu, E.C. Werlin, M. Chen, G. Mottola, A. Chatterjee, K.D. Lance, D.A. Bernards, B.E. Sansbury, M. Spite, T.A. Desai, M.S. Conte, Perivascular delivery of resolvin D1 inhibits neointimal hyperplasia in a rabbit vein graft model, J. Vasc. Surg. 68 (2018) 188S–200S e4.

[12] M.A. Chaudhary, L.W. Guo, X. Shi, G. Chen, S. Gong, B. Liu, K.C. Kent, Periadventitial drug delivery for the prevention of intimal hyperplasia following open surgery, J. Contr. Release 233 (2016) 174–180.

[13] T. Shirasu, N. Yodsanit, J. Li, Y. Huang, X. Xie, R. Tang, Q. Wang, M. Zhang, G. Urabe, A. Webb, Y. Wang, X. Wang, R. Xie, B. Wang, K.C. Kent, S. Gong, L. W. Guo, Neointima abating and endothelium preserving - an adventitia-localized nanoformulation to inhibit the epigenetic writer DOT1L, Biomaterials 301 (2023) 122245.

[14] I. Mylonaki, E. Allemann, F. Saucy, J.A. Haefliger, F. Delie, O. Jordan, Perivascular medical devices and drug delivery systems: making the right choices, Biomaterials 128 (2017) 56–68.

[15] M.S. Conte, D.F. Bandyk, A.W. Clowes, G.L. Moneta, L. Seely, T.J. Lorenz, H. Namini, A.D. Hamdan, S.P. Roddy, M. Belkin, S.A. Berceli, R.J. DeMasi, R. H. Samson, S.S. Berman, P.I. Investigators, Results of PREVENT III: a multicenter, randomized trial of edifoligide for the prevention of vein graft failure in lower extremity bypass surgery, J. Vasc. Surg. 43 (2006) 742–751. ; discussion 751.

[16] A.J.R. Barcena, J.V.D. Perez, O. Liu, A. Mu, F.M. Heralde 3rd, S.Y. Huang, M. P. Melancon, Localized perivascular therapeutic approaches to inhibit venous neointimal hyperplasia in arteriovenous fistula access for hemodialysis use, Biomolecules 12 (2022).

[17] J. Lee, E.H. Jang, J.H. Kim, S. Park, Y. Kang, S. Park, K. Lee, J.H. Kim, Y.N. Youn, W. Ryu, Highly flexible and porous silk fibroin microneedle wraps for perivascular drug delivery, J. Contr. Release : official journal of the Controlled Release Society 340 (2021) 125–135.

[18] T. Shirasu, N. Yodsanit, X. Xie, Y. Zhao, Y. Wang, R. Xie, Y. Huang, B. Wang, G. Urabe, S. Gong, L.W. Guo, K.C. Kent, An adventitial painting modality of local drug delivery to abate intimal hyperplasia, Biomaterials 275 (2021) 120968.

[19] G. Chen, X. Shi, B. Wang, R. Xie, L.W. Guo, S. Gong, K.C. Kent, Unimolecular micelle-based hybrid system for perivascular drug delivery produces long-term efficacy for neointima attenuation in rats, Biomacromolecules 18 (2017) 2205–2213.

[20] X. Shi, G. Chen, L.W. Guo, Y. Si, M. Zhu, S. Pilla, B. Liu, S. Gong, K.C. Kent, Periadventitial application of rapamycin-loaded nanoparticles produces sustained inhibition of vascular restenosis, PLoS One 9 (2014) e89227.

[21] A.K. Singh, C. Cai, S. Kilari, C. Zhao, M.L. Simeon, E. Takahashi, E.R. Edelman, H. J. Kong, T. Macedo, R.J. Singh, M.W. Urban, R. Kumar, S. Misra, 1alpha,25-Dihydroxyvitamin D(3) encapsulated in nanoparticles prevents venous neointimal hyperplasia and stenosis in porcine arteriovenous fistulas, J. Am. Soc. Nephrol. 32 (2021) 866–885.

[22] B. Applewhite, A. Gupta, Y. Wei, X. Yang, L. Martinez, M.G. Rojas, F. Andreopoulos, R.I. Vazquez-Padron, Periadventitial beta-aminopropionitrile-loaded nanofibers reduce fibrosis and improve arteriovenous fistula remodeling in rats, Front Cardiovasc Med 10 (2023) 1124106.

[23] M. Somarathna, P.T. Hwang, R.C. Millican, G.C. Alexander, T. Isayeva-Waldrop, J. A. Sherwood, B.C. Brott, I. Falzon, H. Northrup, Y.T. Shiu, C.J. Stubben, J. Totenhagen, H.W. Jun, T. Lee, Nitric oxide releasing nanomatrix gel treatment inhibits venous intimal hyperplasia and improves vascular remodeling in a rodent arteriovenous fistula, Biomaterials 280 (2022) 121254.

[24] C.D. Owens, Adaptive changes in autogenous vein grafts for arterial reconstruction: clinical implications, J. Vasc. Surg. 51 (2010) 736–746.

[25] I. Xenogiannis, M. Zenati, D.L. Bhatt, S.V. Rao, J. Rodes-Cabau, S. Goldman, K. A. Shunk, K. Mavromatis, S. Banerjee, K. Alaswad, I. Nikolakopoulos, E. Vemmou, J. Karacsonyi, D. Alexopoulos, M.N. Burke, V.N. Bapat, E.S. Brilakis, Saphenous vein graft failure: from pathophysiology to prevention and treatment strategies, Circulation 144 (2021) 728–745.

[26] T. Rajathurai, S.I. Rizvi, H. Lin, G.D. Angelini, A.C. Newby, G.J. Murphy, Periadventitial rapamycin-eluting microbeads promote vein graft disease in long-term pig vein-into-artery interposition grafts, Circ Cardiovasc Interv 3 (2010) 157–165.

[27] Y. Zhu, T. Takayama, B. Wang, A. Kent, M. Zhang, B.Y. Binder, G. Urabe, Y. Shi, D. DiRenzo, S.A. Goel, Y. Zhou, C. Little, D.A. Roenneburg, X.D. Shi, L. Li, W. L. Murphy, K.C. Kent, J. Ke, L.W. Guo, Restenosis inhibition and Re-differentiation of TGFbeta/smad3-activated smooth muscle cells by resveratrol, Sci. Rep. 7 (2017) 41916.

[28] T. Melnik, A. Porcello, F. Saucy, F. Delie, O. Jordan, Bioadhesive perivascular microparticle-gel drug delivery system for intimal hyperplasia prevention: in vitro evaluation and preliminary biocompatibility assessment, Gels 8 (2022).

[29] X. Yu, T. Takayama, S.A. Goel, X. Shi, Y. Zhou, K.C. Kent, W.L. Murphy, L.W. Guo, A rapamycin-releasing perivascular polymeric sheath produces highly effective inhibition of intimal hyperplasia, J. Contr. Release 191 (2014) 47–53.

[30] M. Zhang, B. Wang, G. Urabe, H.G. Ozer, R. Han, K.C. Kent, L.-W. Guo, Angioplasty-induced epigenomic remodeling entails BRD4 and EZH2 hierarchical regulations, bioRxiv (2020). https://dx.doi.org/10.1101/2020.03.12.9896-40.
[31] M. Zhang, J. Li, Q. Wang, G. Urabe, R. Tang, Y. Huang, J.V. Mosquera, K.C. Kent, B. Wang, C.L. Miller, L.W. Guo, Gene-repressing epigenetic reader EED unexpectedly enhances cyclinD1 gene activation, Mol. Ther. Nucleic Acids 31 (2023) 717–729.
[32] Z. Jiang, L. Wu, B.L. Miller, D.R. Goldman, C.M. Fernandez, Z.S. Abouhamze, C. K. Ozaki, S.A. Berceli, A novel vein graft model: adaptation to differential flow environments, Am. J. Physiol. Heart Circ. Physiol. 286 (2004) H240–H245.
[33] P. Yu, B.T. Nguyen, M. Tao, C. Campagna, C.K. Ozaki, Rationale and practical techniques for mouse models of early vein graft adaptations, J. Vasc. Surg. 52 (2010) 444–452.
[34] Z. Jiang, M. Tao, K.A. Omalley, D. Wang, C.K. Ozaki, S.A. Berceli, Established neointimal hyperplasia in vein grafts expands via TGF-beta-mediated progressive fibrosis, Am. J. Physiol. Heart Circ. Physiol. 297 (2009) H1200–H1207.
[35] M.K. Krishnamoorthy, R.K. Banerjee, Y. Wang, J. Zhang, A. Sinha Roy, S.F. Khoury, L.J. Arend, S. Rudich, P. Roy-Chaudhury, Hemodynamic wall shear stress profiles influence the magnitude and pattern of stenosis in a pig AV fistula, Kidney Int. 74 (2008) 1410–1419.
[36] Y. Wang, M. Krishnamoorthy, R. Banerjee, J. Zhang, S. Rudich, C. Holland, L. Arend, P. Roy-Chaudhury, Venous stenosis in a pig arteriovenous fistula model–anatomy, mechanisms and cellular phenotypes, Nephrol. Dial. Transplant. 23 (2008) 525–533, *official publication of the European Dialysis and Transplant Association - European Renal Association*.
[37] Y. Huang, G. Urabe, M. Zhang, J. Li, H.G. Ozer, B. Wang, K.C. Kent, L.W. Guo, Nullifying epigenetic writer DOT1L attenuates neointimal hyperplasia, Atherosclerosis 308 (2020) 22–31.
[38] M. Zhang, G. Urabe, H.G. Ozer, X. Xie, A. Webb, T. Shirasu, J. Li, R. Han, K.C. Kent, B. Wang, L.W. Guo, Angioplasty induces epigenomic remodeling in injured arteries, Life Sci. Alliance 5 (2022).
[39] D.X. Sun, Z. Liu, X.D. Tan, D.X. Cui, B.S. Wang, X.W. Dai, Nanoparticle-mediated local delivery of an antisense TGF-beta1 construct inhibits intimal hyperplasia in autogenous vein grafts in rats, PLoS One 7 (2012) e41857.
[40] Y. Zhou, C. Dai, B. Zhang, J. Ge, Adiponectin prevents restenosis through inhibiting cell proliferation in a rat vein graft model, Arq. Bras. Cardiol. 117 (2021) 1179–1188.
[41] T. Stojanovic, A. El-Sayed Ahmad, V. Didilis, O. Ali, A.F. Popov, B.C. Danner, R. Seipelt, H. Dorge, F.A. Schondube, Extravascular perivenous fibrin support leads to aneurysmal degeneration and intimal hyperplasia in arterialized vein grafts in the rat, Langenbeck's Arch. Surg. 394 (2009) 357–362.
[42] C. Tianshu, G. Congrong, Z. Zhiwei, L. Fei, S. Ayu, Z. Yuanbiao, C. Jing, J. Ge, Rapamycin combined with alpha-cyanoacrylate contributes to inhibiting intimal hyperplasia in rat models, Arq. Bras. Cardiol. 112 (2019) 3–10.
[43] O.H. Iwenofu, R.D. Lackman, A.P. Staddon, D.G. Goodwin, H.M. Haupt, J. S. Brooks, Phospho-S6 ribosomal protein: a potential new predictive sarcoma marker for targeted mTOR therapy, Mod. Pathol. 21 (2008) 231–237.
[44] S. Li, Y. Kong, L. Si, Z. Chi, C. Cui, X. Sheng, J. Guo, Phosphorylation of mTOR and S6RP predicts the efficacy of everolimus in patients with metastatic renal cell carcinoma, BMC Cancer 14 (2014) 376.
[45] B. Wang, M. Zhang, T. Takayama, X. Shi, D.A. Roenneburg, K.C. Kent, L.W. Guo, BET bromodomain blockade mitigates intimal hyperplasia in rat carotid arteries, EBioMedicine 2 (2015) 1650–1661.
[46] A.C. Ostriker, K.A. Martin, Bromodomain blockade for intimal hyperplasia - a good bet? EBioMedicine 2 (2015) 1574–1575.
[47] M.R. Alexander, G.K. Owens, Epigenetic control of smooth muscle cell differentiation and phenotypic switching in vascular development and disease, Annu. Rev. Physiol. 74 (2012) 13–40.
[48] D. Gomez, P. Swiatlowska, G.K. Owens, Epigenetic control of smooth muscle cell identity and lineage memory, Arterioscler. Thromb. Vasc. Biol. 35 (2015) 2508–2516.
[49] M.W.B. Zhang, G. Urabe, X. Shi, L.-W. Guo, Inhibition of the enhancer of zeste homolog family mitigates intimal hyperplasia in rat carotid arteries, Arterioscler. Thromb. Vasc. Biol. 37 (2017/5) A332. A332.
[50] J. Liang, Q. Li, W. Cai, X. Zhang, B. Yang, X. Li, S. Jiang, S. Tian, K. Zhang, H. Song, D. Ai, X. Zhang, C. Wang, Y. Zhu, Inhibition of polycomb repressor complex 2 ameliorates neointimal hyperplasia by suppressing trimethylation of H3K27 in vascular smooth muscle cells, Br. J. Pharmacol. 176 (2019) 3206–3219.
[51] D.Y. Lu, E.Y. Chen, D.J. Wong, K. Yamamoto, C.D. Protack, W.T. Williams, R. Assi, M.R. Hall, N. Sadaghianloo, A. Dardik, Vein graft adaptation and fistula maturation in the arterial environment, J. Surg. Res. 188 (2014) 162–173.
[52] D. Mehta, S.J. George, J.Y. Jeremy, M.B. Izzat, K.M. Southgate, A.J. Bryan, A. C. Newby, G.D. Angelini, External stenting reduces long-term medial and neointimal thickening and platelet derived growth factor expression in a pig model of arteriovenous bypass grafting, Nat. Med. 4 (1998) 235–239.
[53] V. Vijayan, N. Shukla, J.L. Johnson, P. Gadsdon, G.D. Angelini, F.C. Smith, R. Baird, J.Y. Jeremy, Long-term reduction of medial and intimal thickening in porcine saphenous vein grafts with a polyglactin biodegradable external sheath, J. Vasc. Surg. 40 (2004) 1011–1019.
[54] L. Moodley, T. Franz, P. Human, M.F. Wolf, D. Bezuidenhout, J. Scherman, P. Zilla, Protective constriction of coronary vein grafts with knitted nitinol, Eur. J. Cardio. Thorac. Surg. 44 (2013) 64–71.
[55] A. Ehsan, M.J. Mann, G. Dell'Acqua, K. Tamura, R. Braun-Dullaeus, V.J. Dzau, Endothelial healing in vein grafts: proliferative burst unimpaired by genetic therapy of neointimal disease, Circulation 105 (2002) 1686–1692.
[56] M.J. Mann, G.H. Gibbons, P.S. Tsao, H.E. von der Leyen, J.P. Cooke, R. Buitrago, R. Kernoff, V.J. Dzau, Cell cycle inhibition preserves endothelial function in genetically engineered rabbit vein grafts, J. Clin. Invest. 99 (1997) 1295–1301.
[57] D.P. Taggart, C.M. Webb, A. Desouza, R. Yadav, K.M. Channon, F. De Robertis, C. Di Mario, Long-term performance of an external stent for saphenous vein grafts: the VEST IV trial, J. Cardiothorac. Surg. 13 (2018) 117.
[58] M.J. Collins, X. Li, W. Lv, C. Yang, C.D. Protack, A. Muto, C.C. Jadlowiec, C. Shu, A. Dardik, Therapeutic strategies to combat neointimal hyperplasia in vascular grafts, Expert Rev. Cardiovasc Ther. 10 (2012) 635–647.
[59] K. Wadey, J. Lopes, M. Bendeck, S. George, Role of smooth muscle cells in coronary artery bypass grafting failure, Cardiovasc. Res. 114 (2018) 601–610.
[60] R.M. Zwolak, M.C. Adams, A.W. Clowes, Kinetics of vein graft hyperplasia: association with tangential stress, J. Vasc. Surg. 5 (1987) 126–136.
[61] B.J. Cao, X.W. Wang, L. Zhu, R.J. Zou, Z.Q. Lu, Dedicator of cytokinesis 2 silencing therapy inhibits neointima formation and improves blood flow in rat vein grafts, J. Mol. Cell. Cardiol. 128 (2019) 134–144.
[62] V.K. Stark, T.F. Warner, J.R. Hoch, An ultrastructural study of progressive intimal hyperplasia in rat vein grafts, J. Vasc. Surg. 26 (1997) 94–103.
[63] W.J. Gasper, C.D. Owens, J.M. Kim, N. Hills, M. Belkin, M.A. Creager, M.S. Conte, Thirty-day vein remodeling is predictive of midterm graft patency after lower extremity bypass, J. Vasc. Surg. 57 (2013) 9–18.
[64] J. Shelton, D. Wang, H. Gupta, J.M. Wyss, S. Oparil, C.R. White, The neointimal response to endovascular injury is increased in obese Zucker rats, Diabetes Obes. Metabol. 5 (2003) 415–423.
[65] M. Harachi, K. Masui, H. Honda, Y. Muragaki, T. Kawamata, W.K. Cavenee, P. S. Mischel, N. Shibata, Dual regulation of histone methylation by mTOR complexes controls glioblastoma tumor cell growth via EZH2 and SAM, Mol. Cancer Res. 18 (2020) 1142–1152.
[66] M. Espinosa-Martinez, M. Alcazar-Fabra, D. Landeira, The molecular basis of cell memory in mammals: the epigenetic cycle, Sci. Adv. 10 (2024) eadl3188.